

# Recognizing Geometric Intersection Graphs Stabbed by a Line

Dibyayan Chakraborty\*      Kshitij Gajjar†      Irena Rusu‡

September 7, 2022

## Abstract

In this paper, we determine the computational complexity of recognizing two graph classes, grounded L-graphs and stabbable grid intersection graphs. An L-shape is made by joining the bottom end-point of a vertical ( $|$ ) segment to the left end-point of a horizontal ( $-$ ) segment. The top end-point of the vertical segment is known as the *anchor* of the L-shape. Grounded L-graphs are the intersection graphs of L-shapes such that all the L-shapes' anchors lie on the same horizontal line. We show that recognizing grounded L-graphs is NP-complete. This answers an open question asked by Jelínek & Töpfer (Electron. J. Comb., 2019).

Grid intersection graphs are the intersection graphs of axis-parallel line segments in which two vertical (similarly, two horizontal) segments cannot intersect. We say that a (not necessarily axis-parallel) straight line  $\ell$  stabs a segment  $s$ , if  $s$  intersects  $\ell$ . A graph  $G$  is a stabbable grid intersection graph (STABGIG) if there is a grid intersection representation of  $G$  in which the same line stabs all its segments. We show that recognizing STABGIG graphs is NP-complete, even when the input graphs are restricted to be bipartite apex graphs of large (but constant) girth. This answers an open question asked by Chaplick *et al.* (Order, 2018).

## 1 Introduction

Recognizing a graph class means deciding whether a given graph is a member of the graph class. In this paper, we deal with the computational complexity of recognizing intersection graphs of certain types of geometric objects in the plane. These recognition problems stemmed from various fields of active research, like VLSI design [11, 12, 26], map labelling [1], wireless networks [21], computational biology [29], and have now become an indelible part of computational geometry.

Perhaps the most extensively studied class of geometric intersection graphs is the class of *interval graphs* (intersection graphs of intervals on the real line), introduced by Benzer [5] while studying the fine structure of genes. In 1962, Lekkerkerker & Boland [22] proved that the class of interval graphs is precisely the class of graphs without *holes*<sup>1</sup> and *asteroidal triples*<sup>2</sup>. The above elegant result of Lekkerkerker & Boland [22] motivated researchers to study further generalizations of interval graphs and their characterizations. One such generalization was considered by Gyárfás and Lehel [16] who considered the class of *L-intersection graphs*. An *L-shape* [16] is a couple made of a vertical and horizontal segment, whose bottom and left end-points coincide. *L-intersection graphs* are the intersection graphs of L-shapes. Observe that interval graphs can be expressed as intersection graphs of L-shapes as follows: given an interval representation of a graph, replace each interval with an L-shape whose horizontal segment is the same as the interval on the horizontal line  $y = 0$ . The popularity of L-graphs among graph theorists increased when Gonçalves [15] proved that all planar graphs (graphs that can be drawn in the plane

\*Univ Lyon, CNRS, ENS de Lyon, Université Claude Bernard Lyon 1, LIP UMR5668, France

†Indian Institute of Technology Jodhpur, India

‡Nantes Université, École Centrale Nantes, CNRS, LS2N, UMR 6004, F-44000 Nantes, France

<sup>1</sup>A hole is an induced cycle with 4 or more vertices.

<sup>2</sup>Three vertices of a graph form an asteroidal triple if the removal of any one of the vertices (along with all its neighbouring vertices) from the graph does not disconnect the other two.

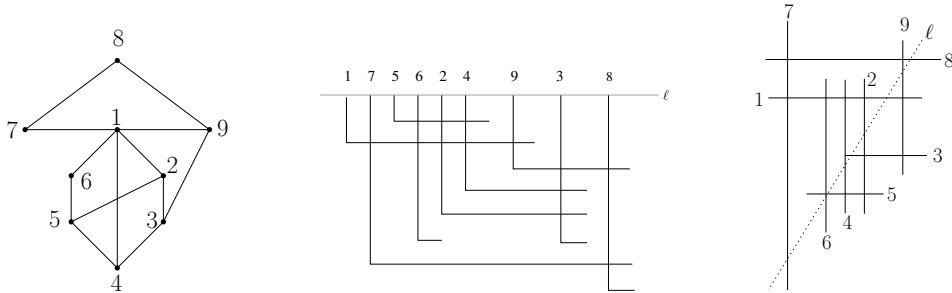


Figure 1: A graph (left) with its grounded L-shape representations (middle) and its stabbable grid intersection representation (right).

in such a way that edges can intersect only at their end-points) are L-graphs. In contrast, recognizing L-graphs is NP-complete even if the inputs are restricted to apex graphs [9] (see Definition 1 below).

An interesting subclass of L-graphs called *infinite-L-graphs* was considered by McGuinness [23]. The top end-point of the vertical segment of an L-shape is called the *anchor* of the L-shape. *Infinite-L-graphs*, also known as *grounded L-graphs* are the intersection graphs of L-shapes whose anchors belong to the same horizontal line, called the *ground line*. See Figure 1 for an example. Interval graphs are (also) grounded L-graphs. (Indeed, given a set of intervals, replace each interval with an L-shape whose horizontal segment is the same as the interval on the horizontal line  $y = 0$  and whose anchor lies on the horizontal line  $y = 1$ ). Other well-studied subclasses of grounded L-graphs are (see [2]) outerplanar graphs, permutation graphs, circle graphs etc. Researchers have studied different aspects (e.g. chromatic number [23, 13], dominating set [8], independent set [7], forbidden patterns [18]) of grounded L-graphs. However, the complexity of recognizing grounded L-graphs remained open. In this paper, we prove that recognizing grounded L-graphs is NP-complete answering a question asked by Jelínek and Töpfer [18].

**Theorem 1.** *Recognizing grounded L-graphs is NP-complete.*

A “two-dimensional” analogue of interval graphs is the class of *rectangle intersection graphs* (i.e., intersection graphs of axis-parallel rectangles in the plane). This graph class was introduced by Asplund & Grünbaum [3] in 1960, who studied the chromatic number of such graphs. After almost three decades, Kratochvíl [19] proved that recognizing rectangle intersection graphs is NP-complete, even if the input graphs are restricted to bipartite graphs. Interestingly, bipartite rectangle intersection graphs are exactly the class of grid intersection graphs (GIG), i.e., intersection graphs of axis-parallel line segments in the plane where no two segments with the same orientation intersect [17]. This implies that the recognition of GIG is NP-complete, and motivates the study of its subclasses. Chaplick *et al.* [10] introduced the class of *stabbable grid intersection graphs*. A segment  $s$  in the plane is *stabbed* by a line  $\ell$  if  $s$  and  $\ell$  intersect. A graph  $G$  is a *stabbable grid intersection graph* (STABGIG) if it has a grid intersection representation such that there exists a straight line that stabs all the segments of the representation. See Figure 1 for an example. All planar bipartite graphs are STABGIGs [14] and Chaplick *et al.* [10] left the problem of recognizing stabbable grid intersection graphs as open. In this paper, we answer their question.

**Definition 1.** [28, 27]. *A graph is an apex graph if it contains a vertex whose removal makes it planar.*

**Theorem 2.** *For every fixed positive integer  $g \geq 10$ , recognizing STABGIG is NP-complete, even when the input graphs are restricted to bipartite apex graphs of girth exactly  $g$ .*

**Organisation:** In Sections 2 and 3, we prove Theorem 1 and Theorem 2, respectively. In Section 4, we conclude.

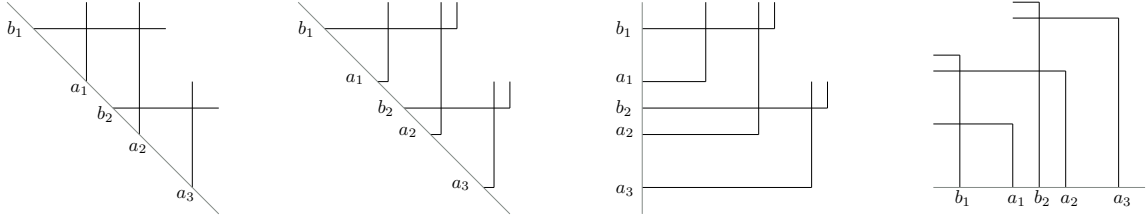


Figure 2: Transforming a stick representation into a grounded  $\Upsilon$ -representation. Here, the stick graph is the induced path  $a_1b_1a_2b_2a_3$ .

**Notations:** For a positive integer  $n \geq 1$ ,  $[n]$  denotes the set  $\{1, 2, \dots, n\}$ . All graphs considered in this paper are simple and undirected. For a graph  $G$ , the sets  $V(G)$  and  $E(G)$  denote the vertex set and edge set of  $G$ , respectively.

**Convention:** Both for grounded L-graphs and StabGIGs, we assume without loss of generality that any two segments in the representation intersect in at most one point. Otherwise, slight changes in the position and length of the segments allow to transform a representation that does not have this property into a convenient one.

## 2 Proof of Theorem 1

In our presentation, the geometrical representation of the grounded L-graphs uses  $\Upsilon$ -shapes above the horizontal ground line rather than L-shapes below it. For a grounded L-graph, this representation is its *grounded  $\Upsilon$ -representation*. Note that the convention above implies that all the anchors are distinct.

The  $\Upsilon$ -shape representing a vertex  $x$  is denoted by  $\Upsilon(x)$ , and the anchor of  $\Upsilon(x)$ , now located at the bottom of the vertical segment, is denoted by  $x$  too. The left to right order of the anchors along the ground line is denoted by  $\prec$ . Note that for two intersecting  $\Upsilon$ -shapes  $\Upsilon(x)$  and  $\Upsilon(y)$ , we have  $x \prec y$  if and only if the vertical segment of  $\Upsilon(x)$  intersects the horizontal segment of  $\Upsilon(y)$ . A  $\Upsilon$ -shape that has intersections only on its vertical (respectively horizontal) segment is called a  $\Upsilon^v$ -*shape* (respectively a  $\Upsilon^h$ -*shape*).

Then the problem we are interested in may be restated as follows:

GROUNDING L-GRAPHS RECOGNITION (GROUNDING L-REC)

**Input:** A graph  $H$ .

**Question:** Is there a grounded  $\Upsilon$ -representation for  $H$ ?

Then Theorem 1 is equivalent to the statement that GROUNDING L-REC is NP-complete.

In order to show it, we use another class of geometric intersection graphs, namely stick graphs. They have been defined in [10] as the intersection graphs of a set  $A$  of vertical segments in the plane and a set  $B$  of horizontal segments in the plane, such that the bottom end-point of the segments in  $A$  and the left end-point of the segments in  $B$  belong to a ground straight line with slope -1. Again, all the endpoints may be considered as distinct. Stick graphs are bipartite graphs, and the aforementioned geometrical representation is called their *stick representation*.

We prove Theorem 1 using a reduction from the problem below, which is NP-complete [25]:

STICK GRAPHS RECOGNITION (STICKREC)

**Input:** A bipartite graph  $G = (A \cup B, E)$ .

**Question:** Is there a Stick representation of  $G$  with sets  $A$  and  $B$ ?

Grounding L-graphs and stick graphs are related by the following relationship, which is essential to our construction.

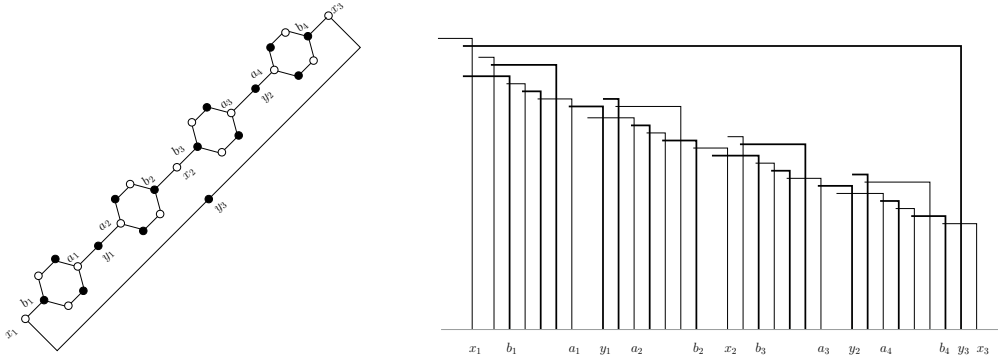


Figure 3: An example of a bipartite grounded L-graph, which is not a stick graph. The bipartition is indicated by the two colours of the vertices, white and black. In the grounded  $\Upsilon$ -representation presented here, the thick  $\Upsilon$ -shapes correspond to the black vertices.

**Proposition 3.** *All stick graphs are grounded L-graphs. Moreover, each stick graph has a grounded  $\Upsilon$ -representation in which the vertices in  $A$  are represented by  $\Upsilon^h$ -shapes, and those in  $B$  by  $\Upsilon^v$ -shapes.*

*Proof.* Let  $G$  be a stick graph. Figure 2 illustrates the steps of the proof. Consider a stick representation of  $G$ , and replace first each vertical (respectively horizontal) segment with a  $\perp$ -shape having the same anchor as the initial segment, whose horizontal (respectively vertical) segment is not used for intersections. Then extend the horizontal segments of the  $\perp$ -shapes towards left so that to place all the anchors on the same vertical line, that becomes the new ground line. Finally, perform a 90 degrees counterclockwise rotation of the whole representation to obtain a grounded  $\Upsilon$ -representation of  $G$ . In this representation, the vertices in  $A$  are represented by  $\Upsilon^h$ -shapes, and those in  $B$  by  $\Upsilon^v$ -shapes.  $\square$

**Remark 1.** *Not all the bipartite grounded L-graphs are stick graphs. The bipartite graph in Figure 3 is not a stick graph [10], but is a grounded L-graph as shown by the  $\Upsilon$ -representation we provide.*

## 2.1 The reduction

Our reduction from STICKREC to GROUNDED L-REC strongly relies on Proposition 3. It transforms a given bipartite graph  $G = (A \cup B, E)$  into a (non-bipartite) graph  $H$  that is roughly a copy of  $G$  where each vertex  $x$  from  $B$  is placed inside a gadget graph called  $\Lambda(x)$ . The role of the gadgets is to force the grounded  $\Upsilon$ -representation of  $G$  produced inside any grounded  $\Upsilon$ -representation of  $H$  (if any) to be stick-like, that is, to represent the vertices in  $A$  by  $\Upsilon^h$ -shapes and the vertices in  $B$  by  $\Upsilon^v$ -shapes. In this way, a grounded  $\Upsilon$ -representation exists for  $H$  if and only if a stick representation exists for  $G$ .

More formally, let  $\Lambda(x)$  be the graph in Figure 4 (left). Consider an instance  $G = (A \cup B, E)$  of STICKREC, and build an instance  $H$  of GROUNDED L-REC as follows:

1. for each  $a \in A$ , define a vertex  $a$  of  $H$ .
2. for each  $b \in B$ , consider a copy of  $\Lambda(b)$  such that for each pair  $b \neq b'$ , the graphs  $\Lambda(b)$  and  $\Lambda(b')$  are disjoint.
3. for each edge  $ab \in E$  with  $a \in A$  and  $b \in B$ , add an edge from  $a$  to every vertex in  $\Lambda(b)$ .

See Figure 4 (right) for an example. We show in the next section that this reduction proves the NP-completeness of GROUNDED L-REC.

## 2.2 The proofs

The gadget  $\Lambda(x)$  has been chosen so as to have very few and convenient grounded  $\Upsilon$ -representations.

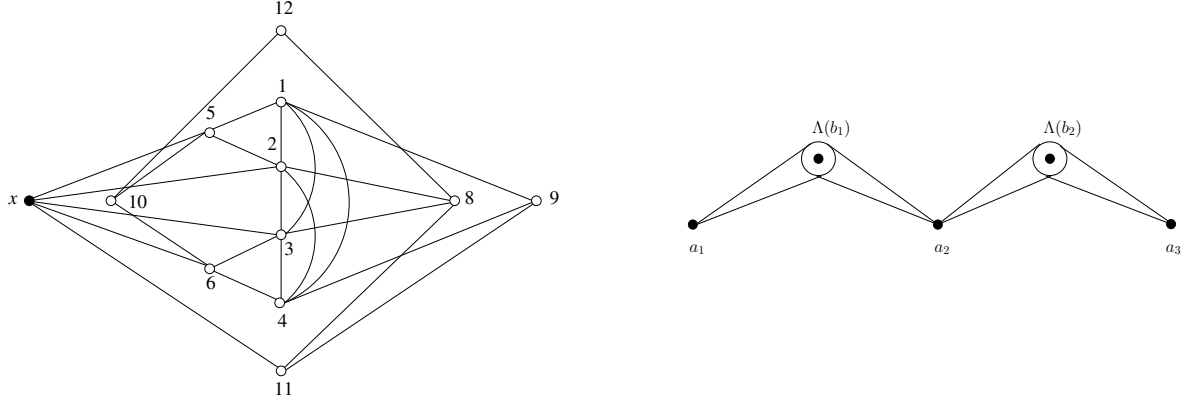


Figure 4: The graph  $\Lambda(x)$  (left) and the construction of the graph  $H$  when  $G$  is the path  $a_1b_1a_2b_2a_3$  (right).

**Proposition 4.** *The graph  $\Lambda(x)$  is a grounded  $\mathbb{L}$ -graph. It admits exactly two grounded  $\mathbb{T}$ -representations, given in Figures 5(a) and 5(b).*

*Proof.* The proof consists of a case study. The vertices 1, 2, 3, 4 induce a complete subgraph, whose grounded  $\mathbb{T}$ -representation is unique up to the labelling of the anchors. It consists of four  $\mathbb{T}$ -shapes whose anchors are ordered from left to right along the ground line, such that the horizontal segment of each  $\mathbb{T}$ -shape intersects the vertical segments of all the  $\mathbb{T}$ -shapes located to its left. The four anchors may be labelled from left to right with any permutation  $\pi$  of 1, 2, 3, 4. Taking into account the symmetry between the (ordered) triplets (1, 2, 5) and (4, 3, 6) we can reduce the number of permutations to the 12 of them whose leftmost element is 1 or 2. Once a permutation  $\pi$  is fixed, several (at most three) subcases appear depending on the position of the anchor of  $\mathbb{T}(5)$ . As the grounded  $\mathbb{T}$ -representation is progressively completed by adding  $\mathbb{T}$ -shapes corresponding to new vertices, all of the representations but one fail to place all the anchors. Below, the numbers correspond to anchors, and it is assumed that the reader draws himself the exact form of each  $\mathbb{T}$ -shape so that only the correct intersections occur. We also assume that the  $\mathbb{T}$ -shapes for the anchors 1, 2, 3, 4 are already drawn according to the order given by  $\pi$ .

- $\pi = 1234$ . a) When  $5 \prec 1$ , there are three possible positions for 6, but none of them allows to place  $x$ . b) When  $2 \prec 5 \prec 3$ , there are four possible positions for 6, but when  $3 \prec 6 \prec 4$  there is no possible place for 10, and when  $6 \prec 1$ , there is no place for  $x$ . When  $5 \prec 6 \prec 3$  or  $4 \prec 6$ , the anchor  $x$  is placed either before 1 (when  $5 \prec 6 \prec 3$ ) or between 3 and 4 (for both positions of 6). When  $x \prec 1$ , there is no way to place 9. Then we must have  $3 \prec x \prec 4$ , in which case we have  $8 \prec 1$  (for both positions of 6) or  $6 \prec 8$  (only when  $1 \prec 6$ ), and thus there is no possible place for the anchor 11 such that  $\mathbb{T}(11)$  intersects  $\mathbb{T}(x)$  and  $\mathbb{T}(8)$  but none of  $\mathbb{T}(1)$ ,  $\mathbb{T}(2)$ ,  $\mathbb{T}(3)$ ,  $\mathbb{T}(4)$ . c) When  $4 \prec 5$ , there are four possible positions for 6, but there is no way to place  $x$  when  $4 \prec 6 \prec 5$ . When  $2 \prec 6 \prec 3$  or  $3 \prec 6 \prec 4$ , we necessarily have  $5 \prec x$ ,  $9 \prec 1$  and  $3 \prec 8 \prec 6$  (possible only when  $3 \prec 6 \prec 4$ ). Then 11 cannot be placed. When  $6 \prec 1$ , we necessarily have  $x \prec 6$  and  $1 \prec 9 \prec 2$ , which leaves no place for 11.
- $\pi = 1243$ . a) When  $5 \prec 1$ , among the four possible positions for 6 only  $5 \prec 6 \prec 1$  allows finding a place for  $x$  (between 5 and 6). But then 9 cannot be placed. b) When  $2 \prec 5 \prec 4$ , there are four possible positions for 6. When  $6 \prec 1$ , one cannot find a position for  $x$ . When  $5 \prec 6 \prec 4$ , we have  $x \prec 1$ , and there is no available position for 9. When  $4 \prec 6 \prec 3$  or  $3 \prec 6$ , we can find a position for  $x$  (between 2 and 5). Then the unique possible position for 9, satisfying  $9 \prec 1$ , does not allow us to find a position for 11. c) When  $3 \prec 5$ , the position of 6 between 2 and 4 does not allow to place  $x$ . When  $6 \prec 1$ , we must have  $x \prec 6$ , and then 9 cannot be placed. Finally, when  $4 \prec 6 \prec 3$  or  $3 \prec 6 \prec 5$ , we necessarily have  $4 \prec x \prec 3$  and  $9 \prec 1$ , so there is no appropriate place for 11.
- $\pi = 1324$ . In this case, we deduce  $5 \prec 1$  and  $2 \prec 6 \prec 4$ , and 10 cannot be placed.

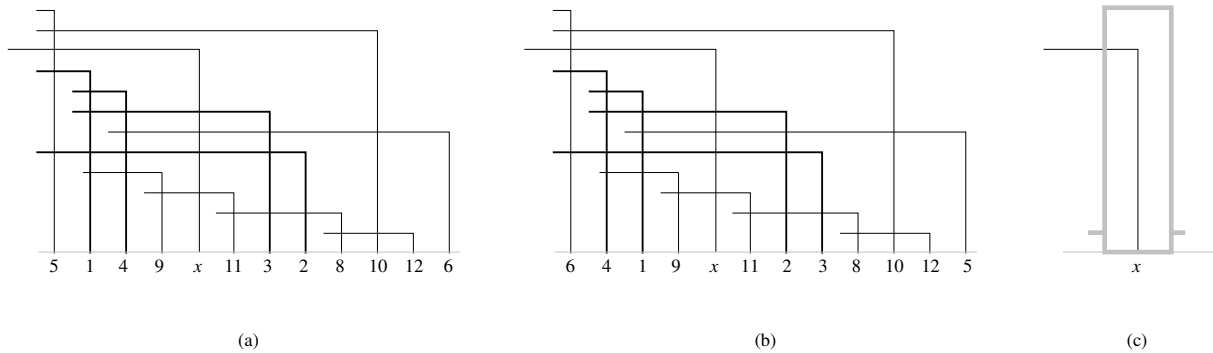


Figure 5: (a)(b) The two grounded  $\gamma$ -representations of  $\Lambda(x)$ . The second one is obtained from the first one by the following renumbering: switch the numbers 1 and 4, then switch the numbers 2 and 3, and finally switch the numbers 5 and 6. (c) The drawing replaces each of them, when only  $\gamma(x)$  and the level of the lowest horizontal segment need to be known.

- $\pi = 1342$ . a) When  $5 \prec 1$ , we have two possible positions for 6, but none of them allows us to place  $x$ . b) When  $1 \prec 5 \prec 3$ , there are three possible positions for 6, namely  $4 \prec 6 \prec 2$  and  $2 \prec 6$ , and both of them allow to place  $x$  (between 3 and 4). There is a unique position for 9, namely  $9 \prec 1$ , and then 11 cannot be placed. c) When  $4 \prec 5 \prec 2$ , there are two possible positions for 6, none of which allows to place  $x$ .
- $\pi = 1423$ . Then  $5 \prec 1$  and  $2 \prec 6 \prec 3$ , and 10 cannot be placed.
- $\pi = 1432$ . a) When  $5 \prec 1$ , we have either  $3 \prec 6 \prec 2$  or  $2 \prec 6$ . In the former case, there is no possibility to place 10, so we necessarily have  $2 \prec 6$ , in which case  $2 \prec 10 \prec 6$ . We also have unique positions for  $x$  and 9, with  $4 \prec x \prec 3$  and  $4 \prec 9 \prec x$ . There are three possible positions for 8, namely:  $5 \prec 8 \prec 1$ ,  $3 \prec 8 \prec 2$  and  $2 \prec 8 \prec 10$ . Only  $2 \prec 8 \prec 10$  allows to place 11, whose  $\gamma$ -shape must intersect  $\gamma(x)$ ,  $\gamma(8)$  and  $\gamma(9)$ , and then  $x \prec 11 \prec 3$ . Then 12 is placed between 10 and 6. This is the unique grounded  $\gamma$ -representation of  $\Lambda(x)$  when symmetry is left apart and it is illustrated in Figure 5(a). b) When  $1 \prec 5 \prec 4$ , we have  $6 \prec 1$ ,  $3 \prec 6 \prec 2$  or  $2 \prec 6$ . The latter case does not allow to find a position for 10. The case  $3 \prec 6 \prec 2$  does not allow finding a position for  $x$ . Then we must have  $6 \prec 1$  and thus  $6 \prec x \prec 1$ , since this is the only possible choice for  $x$ . Then  $9 \prec 6$  is the only place for 9 that allows a position for 11, which must satisfy  $9 \prec 11 \prec 6$ . But then 8 cannot be placed such as  $\gamma(8)$  intersects  $\gamma(x)$ ,  $\gamma(9)$ ,  $\gamma(11)$ ,  $\gamma(2)$  and  $\gamma(3)$ . c) When  $3 \prec 5 \prec 2$ , two cases occur for 6. When  $6 \prec 1$ , we have  $4 \prec x \prec 3$ ,  $4 \prec 9 \prec x$  and either  $6 \prec 8 \prec 1$  or  $3 \prec 8 \prec 5$ . None of the cases allows placing 11. When  $3 \prec 6 \prec 5$ , we have again  $4 \prec x \prec 3$ . We also have  $8 \prec 1$  or  $6 \prec 8 \prec 5$ , and either  $9 \prec 1$  (and even  $9 \prec 8 \prec 1$  in the former case) or  $4 \prec 9 \prec x$ . In all cases, there is no place for 11.
- $\pi = 2134$ . a) When  $5 \prec 2$ , there are four possible positions for 6, but none of them allows to place  $x$ . b) When  $1 \prec 5 \prec 3$ , the unique position of 6 that allows placing  $x$  is  $5 \prec 6 \prec 3$ . In this case, we have  $x \prec 2$  and 9 must satisfy  $5 \prec 9 \prec 6$ . But then there is no appropriate place for 11. c) When  $4 \prec 5$ , among the four possible positions for 6 only  $6 \prec 2$  allows to find a place for  $x$ , which satisfies then  $x \prec 6$ . Then  $3 \prec 9 \prec 4$  and 11 cannot be placed.
- $\pi = 2143$ . a) When  $5 \prec 2$ , three cases occur. With  $5 \prec 6 \prec 2$ , we deduce that  $2 \prec x \prec 1$  and 10 satisfies  $6 \prec 10 \prec 2$ . Then either  $2 \prec 8 \prec x$  or  $4 \prec 8 \prec 3$ , and in both cases 12 cannot be placed. With  $4 \prec 6 \prec 3$ , there is no possible place for 10. With  $1 \prec 6 \prec 4$  or  $3 \prec 6$ , we have  $4 \prec x \prec 3$ . Moreover, with  $2 \prec 8 \prec 1$  one cannot find a position for 11, so that we must have  $x \prec 8 \prec 3$ , thus forbidding the position of 6 to the right of 3 (since  $\gamma(8)$  and  $\gamma(6)$  do not intersect). But then there is no possible place for 10. b) When  $1 \prec 5 \prec 4$ ,  $x$  must be to the left of 1, otherwise  $\gamma(x)$  cannot intersect  $\gamma(2)$ ,  $\gamma(3)$  and  $\gamma(5)$ . Then  $6 \prec 2$  is the only appropriate position for 6, and it implies

$2 \prec x \prec 1$ , and  $6 \prec 10 \prec 2$ . Concerning 8, the position  $8 \prec 6$  does not allow to place 11, so only  $4 \prec 8 \prec 3$  is possible. Then there is no possible place for 12. c) When  $3 \prec 5$ , among the 4 possible positions for 6 the one with  $1 \prec 6 \prec 4$  does not allow to find a position for  $x$ . When  $6 \prec 2$ , we must have  $x \prec 6$  and either  $4 \prec 9 \prec 3$  or  $3 \prec 9 \prec 5$ . Then there is no appropriate place for 11. When  $4 \prec 6 \prec 3$  or  $3 \prec 6 \prec 5$ , we have  $4 \prec x \prec 3$  (and even  $4 \prec x \prec 6 \prec 3$  when 6 is between 4 and 3) and either  $8 \prec 2$  or  $2 \prec 8 \prec 1$ . None of them allows placing 11.

- $\pi = 2314$ . Then  $5 \prec 2$ ,  $1 \prec 6 \prec 4$  and 10 cannot be placed.
- $\pi = 2341$ . a) When  $5 \prec 2$ , we cannot have  $4 \prec 6 \prec 1$  since there is no available position for 10, so we necessarily have  $1 \prec 6$  and  $1 \prec 10 \prec 6$ . The only possible places for  $x$  and 8 satisfy  $1 \prec x \prec 10$  and  $3 \prec 8 \prec 4$ . But then 11 cannot be placed. b) When  $2 \prec 5 \prec 3$ , three positions exist for 6, with  $6 \prec 2$ ,  $4 \prec 6 \prec 1$  and  $1 \prec 6$ . The latter one does not allow placing 10. For the two former cases, we have  $3 \prec x \prec 4$ . But then when  $6 \prec 2$ , there is no appropriate place for 10. We deduce that  $4 \prec 6 \prec 1$ , and thus there is a unique place for 10, such that  $5 \prec 10 \prec 3$ . Concerning 8, the two positions satisfying  $8 \prec 2$  and respectively  $1 \prec 8$  are correct, but none of them allows to find a position for 12. c) When  $4 \prec 5 \prec 1$ , only two positions are appropriate for 6:  $6 \prec 2$  and  $4 \prec 6 \prec 5$ . The latter one does not allow to find a place for  $x$ , so we necessarily have  $6 \prec 2$ , and thus  $10 \prec 6$ . Then there is a unique position for 8, with  $3 \prec 8 \prec 4$ , and it is impossible to find a place for 12.
- $\pi = 2413$ . We deduce that  $5 \prec 2$  and  $1 \prec 6 \prec 3$ , and therefore 10 cannot be placed.
- $\pi = 2431$ . a) When  $5 \prec 2$ , we deduce that  $1 \prec 6$  or  $3 \prec 6 \prec 1$ . In both cases,  $x$  cannot be placed. b) When  $2 \prec 5 \prec 4$ , none of the three positions that are possible for 6 allows to find a place for  $x$ . c) When  $3 \prec 5 \prec 1$ , we have either  $6 \prec 2$  or  $3 \prec 6 \prec 5$ . When  $3 \prec 6 \prec 5$ , there is no place for  $x$ . When  $6 \prec 2$ , we must have  $x \prec 6$  and  $8 \prec x$ , so that it is not possible to find a place for 10.

Thus there is precisely one grounded  $\Upsilon$ -representation when  $\pi$  is one of the 12 permutations whose leftmost value is either 1 or 2. This grounded  $\Upsilon$ -representation is obtained with  $\pi = 1432$  in case a), *i.e.*, with  $5 \prec 1$ . Figure 5(a) illustrates it. Because of the symmetry between the triplets  $(1, 2, 5)$  and  $(4, 3, 6)$ , exactly one other grounded  $\Upsilon$ -representation is possible. It occurs in the case  $\pi = 4123$  and is obtained by simultaneously switching the labels of *all* the pairs of symmetric vertices, namely 1 and 4, 2 and 3, as well as 5 and 6. It is illustrated in Figure 5(b).  $\square$

**Convention.** In the remainder of the proof, each of the grounded  $\Upsilon$ -representations in Figures 5(a) and 5(b) is drawn as a grey box around  $\Upsilon(x)$ , together with two short lateral segments indicating the level of the lowest horizontal segment in the representation. See Figure 5(c).

Let  $\Lambda(x) + u$  be the graph obtained by adding to  $\Lambda(x)$  a new vertex  $u$  adjacent to all the vertices in  $\Lambda(x)$ . Then  $u$  is called *universal* with respect to  $\Lambda(x)$ .

**Proposition 5.** *The graph  $\Lambda(x) + u$  is a grounded L-graph. In its two grounded  $\Upsilon$ -representations,  $u$  is the rightmost anchor and thus  $\Upsilon(u)$  is a  $\Upsilon^h$ -shape.*

*Proof.* A grounded  $\Upsilon$ -representation of  $\Lambda(x) + u$  is obtained by placing the anchor of  $u$  to the extreme right of the grounded  $\Upsilon$ -representation of  $\Lambda(x)$ , and letting the horizontal segment of  $\Upsilon(u)$  intersect the vertical segments of all the other  $\Upsilon$ -shapes at a very low height (lower than the horizontal segment of  $\Upsilon(12)$ ). Then  $\Upsilon(u)$  is a  $\Upsilon^h$ -shape. The conclusion of Proposition 5 is reached by noticing that, with the  $\Upsilon$ -representation in Figure 5(a), any possible alternate position for  $u$  necessarily belongs to the interval defined by 2 and 8 (so that  $\Upsilon(6)$ ,  $\Upsilon(12)$ ,  $\Upsilon(10)$  and  $\Upsilon(8)$  can be intersected by  $\Upsilon(u)$ ), but then  $\Upsilon(u)$  cannot intersect  $\Upsilon(2)$ .  $\square$

**Proposition 6.** *The graph  $G$  is a yes-instance of STICKREC if and only if the graph  $H$  is a yes-instance of GROUNDED L-REC.*

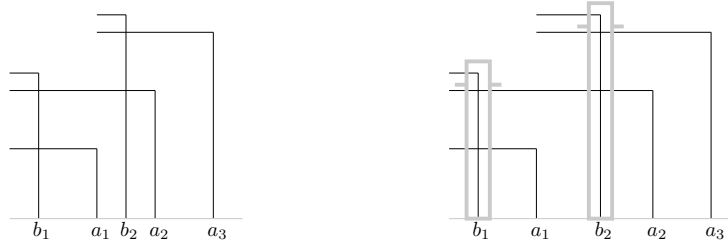


Figure 6: The grounded  $\Upsilon$ -representation of  $G$  (left) and the grounded  $\Upsilon$ -representation of  $H$  (right), when  $G$  is the induced path  $a_1b_1a_2b_2a_3$  (right).

*Proof.* For the forward direction, Proposition 3 implies that the stick graph  $G$  has a grounded  $\Upsilon$ -representation. We transform this representation of  $G$  into a grounded  $\Upsilon$ -representation of  $H$  as follows. For each  $b \in B$ , build a grounded  $\Upsilon$ -representation of  $\Lambda(b)$  (whose existence is ensured by Proposition 4) as a block, in the immediate neighborhood of  $\Upsilon(b)$ . See Figure 6. The lowest horizontal segment of a  $\Upsilon$ -shape in this grounded  $\Upsilon$ -representation of  $\Lambda(b)$ , indicated in the figure by the two grey lateral segments of the grey box, must be placed above all the horizontal segments of  $\Upsilon$ -shapes  $\Upsilon(a)$  with  $a \in A$  and  $ab \in E$ . This is always possible, by increasing the lengths of the vertical segments as needed. Furthermore, for each  $a \in A$  such that  $ab \in E$ , extend the horizontal segment of  $\Upsilon(a)$  such that it intersects all the  $\Upsilon$ -shapes representing vertices in  $\Lambda(b)$ . The resulting grounded  $\Upsilon$ -representation is a grounded  $\Upsilon$ -representation of  $H$ .

We now consider the backward direction and assume that we have a grounded  $\Upsilon$ -representation for  $H$ . Let  $a \in A, b \in B$  such that  $ab \in E$ . By the construction of  $H$ ,  $a$  is universal for  $\Lambda(b)$ . By Proposition 5, we deduce that  $\Upsilon(a)$  is a  $\Upsilon^h$ -shape when only the subgraph  $\Lambda(b) + a$  of  $H$  is considered. It follows that the intersection between  $\Upsilon(b)$  and  $\Upsilon(a)$  holds on the vertical segment of  $\Upsilon(b)$ , and on the horizontal segment of  $\Upsilon(a)$ , for each pair  $a \in A, b \in B$  such that  $ab \in E$ . Then the grounded  $\Upsilon$ -representation of  $G$  may be transformed into a stick-representation of  $G$  by successively transforming the horizontal ground line into a vertical ground line, and then into a ground line with slope -1, and by finally removing the unused segments (just following the steps in Figure 2 in the reverse order).  $\square$

Now, we are ready to prove that GROUNDED L-REC is NP-complete.

*Proof.* (of Theorem 1). According to [20], and since the number of directions of the segments in the representation is fixed, GROUNDED L-REC is in NP. Proposition 6 shows that our reduction is correct. Moreover, it takes linear time to build  $H$  knowing  $G$ , so that the reduction is polynomial.  $\square$

### 3 Proof of Theorem 2

In this section, we focus on the following problem:

STABBABLE GRID INTERSECTION GRAPHS RECOGNITION (STABGIGREC)

**Input:** A bipartite graph  $G$ .

**Question:** Is there a grid intersection representation of  $G$  in which all segments are stabbed by the same straight line?

Theorem 2 claims that STABGIGREC is NP-complete even when the input graphs are restricted to bipartite apex graphs of girth  $g$ , for any given positive integer  $g \geq 10$ . Our proof technique is similar to that of Chakraborty & Gajjar [9]. As in their proof, we use a reduction from the problem below. A *Hamiltonian path* in a graph is a path that visits each vertex of the graph exactly once.



PLANAR HAMILTONIAN PATH COMPLETION PROBLEM (PHPC)

**Input:** A planar graph  $G$ .

**Question:** Is  $G$  a subgraph of a planar graph with a Hamiltonian path?

### 3.1 The reduction

**Convention.** Throughout our proof, we will assume that  $G$  is a connected graph with at least five vertices, as every graph on four vertices is planar and the planarity of a non-connected graph is reduced to that of its components.

Let  $k$  be a fixed positive odd number. Given a planar graph  $P$  on  $p \geq 5$  vertices, we construct a bipartite apex graph  $P_{k\text{-div}}^{\text{apex}}$  in  $\text{poly}(p)$  time as follows.

Let  $P_{k\text{-div}}$  be the full  $k$ -subdivision of  $P$ , *i.e.*,  $P_{k\text{-div}}$  is the graph obtained by replacing each edge of  $P$  with a path of length  $k + 1$ . Formally, we replace each  $e = xy \in E(P)$  with the path  $(x, u_e^1, u_e^2, \dots, u_e^k, y)$  (see Figure 7).

$$\begin{aligned} V(P_{k\text{-div}}) &= V(P) \cup \{u_e^1, u_e^2, \dots, u_e^k \mid e \in E(P)\}; \\ E(P_{k\text{-div}}) &= \{xu_e^1, u_e^1u_e^2, \dots, u_e^ku_e^k \mid e = xy \in E(P)\}. \end{aligned}$$

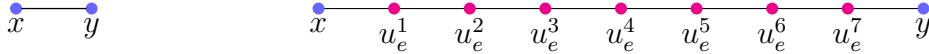


Figure 7: An edge  $e = xy$  (left) and a 7-subdivision of  $e$  (right).

We call the vertices of  $V(P) \subseteq V(P_{k\text{-div}})$  as the *original vertices* of  $P_{k\text{-div}}$  and the remaining vertices as the *subdivision vertices* of  $P_{k\text{-div}}$ . Finally, we construct  $P_{k\text{-div}}^{\text{apex}}$  by adding a new vertex  $a$  (called the ‘apex’) to  $P_{k\text{-div}}$  and making it adjacent to all the original vertices of  $P_{k\text{-div}}$ . Formally,  $P_{k\text{-div}}^{\text{apex}}$  is defined as follows.

$$\begin{aligned} V(P_{k\text{-div}}^{\text{apex}}) &= V(P_{k\text{-div}}) \cup \{a\}; \\ E(P_{k\text{-div}}^{\text{apex}}) &= E(P_{k\text{-div}}) \cup \{av \mid v \in V(P)\}. \end{aligned}$$

The reduction from PHPC to STABGIGREC associates to the planar graph  $G$ , the input of PHPC, the graph  $G_{k\text{-div}}^{\text{apex}}$  built as above, with  $P = G$  and  $k$  an arbitrary but fixed odd integer such that  $k \geq 7$ . See Figure 8 for an example of the reduction. We have:

**Observation 7** ([9]). *If  $G$  is a connected planar graph and  $g, k$  are positive integers such that  $k$  is odd and  $k = g - 3 \geq 3$ , then  $G_{k\text{-div}}^{\text{apex}}$  is a bipartite apex graph of girth exactly  $g$ .*

The graph  $G_{k\text{-div}}^{\text{apex}}$  thus has the properties required in Theorem 2 (which requires  $g \geq 10$ , thus  $k = g - 3 \geq 7$ ). Moreover, the proposition below holds, and will significantly shorten the proof of our theorem. A graph is a *1-string graph* if it is the intersection graph of simple curves in the plane, also called *strings*, such that any two strings intersect at most once, and whenever they intersect they cross each other.

**Proposition 8** ([9]). *Let  $k \geq 3$  be an odd integer. If  $G_{k\text{-div}}^{\text{apex}}$  is a 1-string graph, then  $G$  is a yes-instance of PHPC.*

### 3.2 The proofs

We need to prove that  $G$  is a yes-instance of PHPC if and only if  $G_{k\text{-div}}^{\text{apex}}$  is a yes-instance of STABGIGREC. This section presents the forward direction.

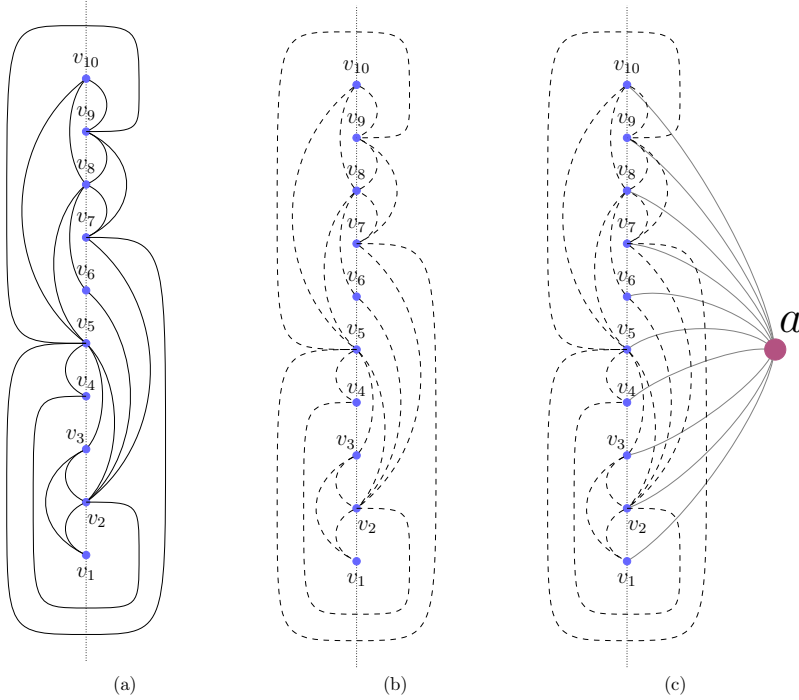


Figure 8: (a) An example graph  $G$  which is a yes-instance of PHPC. (b) Each edge of the graph is replaced with a path with  $k + 1$  edges, where  $k \geq 7$ . (A dashed curve indicates a path of length  $k + 1$ .) (c) The apex graph  $G_{k\text{-div}}^{\text{apex}}$ , constructed by adding one extra vertex (the apex vertex  $a$ ) in  $G_{k\text{-div}}$ .

**Proposition 9.** *Let  $k \geq 7$  be an odd integer. If  $G$  is a yes-instance of PHPC, then  $G_{k\text{-div}}^{\text{apex}}$  is a STABGIG.*

The proof of this result is presented in Sections 3.2.1 to 3.2.3. Section 3.2.4 contains the proof of Theorem 2.

We use the notation  $(x, y)$ , where  $x$  and  $y$  are real values, for the Cartesian coordinates of a point, and the notation  $[(x_1, y_1), (x_2, y_2)]$  for the segment whose endpoints are  $(x_1, y_1)$  and  $(x_2, y_2)$ .

### 3.2.1 Overview of the construction

In view of proving Proposition 9, let  $V(G) = \{v_1, v_2, \dots, v_n\}$ . We start with a plane drawing of  $G$ , *i.e.*, a drawing of  $G$  in the plane, in which the vertices are points and the edges are strings (that is, simple curves). Then we modify the drawing in a step-by-step manner to end with a STABGIG representation of  $G_{k\text{-div}}^{\text{apex}}$ . Let us now provide an overview of these steps.

- (a) Consider a drawing of  $G$  in the plane in which the vertex  $v_i$  (for every  $i \in [n]$ ) has the Cartesian coordinate  $(0, i - 1)$ , each edge of  $G$  crosses the  $y$ -axis (the line  $x = 0$ ) at most once, and no edge of  $G$  crosses the  $y$ -axis between  $y = 0$  and  $y = n - 1$ . (Auer & Gleißner [4] show that such a drawing exists for every graph that is a yes-instance of PHPC.) See Figure 8(a) for an illustration, where  $v_1$  is located at  $(0, 0)$  and  $v_{10}$  is located at  $(0, 9)$ .
- (b) In this drawing, though no edge of  $G$  crosses the  $y$ -axis between the points  $(0, 0)$  and  $(0, n - 1)$ , there might be edges of  $G$  that cross the  $y$ -axis below  $y = 0$  or above  $y = n - 1$ . We place new vertices on the intersection points of those edges with the  $y$ -axis, to create a new graph  $H$ . Let  $n_H$  be the number of vertices in  $H$ . See Figure 9 for an illustration, where there are three such vertices, indicated by square nodes.
- (c) The graph  $H$  has some nice properties. Firstly,  $n \leq n_H \leq 4n$ . Secondly,  $H$  is a subdivision of  $G$ . As subdivision does not affect planarity,  $H$  is also planar. Thirdly, the drawing of  $H$  ensures that

no edge of  $H$  crosses the  $y$ -axis. We fix the line  $y = x$  as our stab line  $\ell$  (recall that  $\ell$  does need not to be axis-parallel), and use the current plane drawing of  $H$  to devise a STABGIG representation of the graph  $H_{3\text{-div}}^{\text{apex}}$ . (The graph  $H_{3\text{-div}}^{\text{apex}}$  is obtained as described in the previous section, by considering  $P = H$  and  $k = 3$ . See Figure 9.) Note that the graph  $G_{k\text{-div}}^{\text{apex}}$  is obtained from  $H_{3\text{-div}}^{\text{apex}}$  by further subdividing some of its edges.

- (d) In the STABGIG representation of  $H_{3\text{-div}}^{\text{apex}}$ , the apex segment of  $H_{3\text{-div}}^{\text{apex}}$  is represented by a long vertical segment coinciding with the  $y$ -axis. The  $n_H$  original vertices of  $H_{3\text{-div}}^{\text{apex}}$  are represented by  $n_H$  horizontal segments, each one crossing the  $y$ -axis at the point defined by its corresponding vertex in the plane representation of  $H$ . Each edge  $e = xy$  of  $H$  (which is a string in the plane drawing of  $H$ ) becomes a path with three intermediate vertices  $u_e^1, u_e^2, u_e^3$  in  $H_{3\text{-div}}^{\text{apex}}$ . These three vertices are represented as three segments that form a  $\sqcup$ -shape or a  $\sqcap$ -shape, whose two vertical segments appropriately intersect the horizontal segments representing respectively  $x$  and  $y$ . See Figure 10 for an illustration (formal details are given below).
- (e) So far, our construction is similar to the construction in [9]. But now, we have to slightly deviate from it. For each edge  $e$  of  $H$ , we need to very precisely and carefully describe the positions of the three segments corresponding to its three subdivision vertices (which will form a  $\sqcup$ -shape or a  $\sqcap$ -shape)  $u_e^1, u_e^2, u_e^3$  in  $H_{3\text{-div}}^{\text{apex}}$ , in such a way that all the three segments intersect the stab line  $\ell$ . This is the most novel and non-trivial part of our proof. See Figure 10 for an illustration.
- (f) Lastly, we need to convert  $H_{3\text{-div}}^{\text{apex}}$  to  $G_{k\text{-div}}^{\text{apex}}$ . Note that  $H_{3\text{-div}}^{\text{apex}} \setminus \{a\}$  is a subdivision of  $G$  in which each edge of  $G$  is subdivided either 3 or 7 times. It is easy to add more segments to the STABGIG representation to ensure that all the edges of  $G$  are subdivided exactly  $k$  times, for any odd number  $k \geq 7$ . An overview of this construction is illustrated by Figure 11. Finally, with the apex segment  $[(0, 0), (0, n - 1)]$ , we have a STABGIG representation of  $G_{k\text{-div}}^{\text{apex}}$ .

### 3.2.2 Construction of $H_{3\text{-div}}^{\text{apex}}$ and its STABGIG representation

Now we commence with the formal proof of Proposition 9. Let us start with item (a). Since  $G$  is a yes-instance of PHPC, according to Auer & Gleißner [4], the edge set  $E(G)$  can be partitioned into three sets  $E_{\text{left}}(G)$ ,  $E_{\text{right}}(G)$ , and  $E_{\text{cross}}(G)$ , such that  $G$  admits a plane drawing satisfying the following properties.

- For every  $i \in [n]$ , the vertex  $v_i$  has the Cartesian coordinate  $(0, i - 1)$ .
- Every edge  $e \in E_{\text{left}}(G)$  lies in the half-plane  $x \leq 0$ .
- Every edge  $e \in E_{\text{right}}(G)$  lies in the half-plane  $x \geq 0$ .
- Every edge  $e \in E_{\text{cross}}(G)$  crosses the line  $x = 0$  exactly once, at  $(0, Y_e)$ , where  $Y_e < 0$  or  $Y_e > n - 1$ .

Figure 8(a) presents an example of a graph, and of a plane drawing of it which satisfies the above properties. Note that the above plane drawing crucially uses the fact that the line  $x = 0$  partitions the plane into two half-planes ( $x \leq 0$  and  $x \geq 0$ ). Now, let us move on to item (b).

The construction of  $H$  from  $G$  is done as follows. For each edge  $e = v_i v_j \in E_{\text{cross}}(G)$ , we add a new vertex  $\text{new}_e$  to the graph, represented by the point  $(0, Y_e)$ . Consequently, the edge  $e = v_i v_j$  is replaced by two edges  $v_i \text{new}_e$  and  $\text{new}_e v_j$ . One of those edges is in  $E_{\text{left}}(H)$  and the other is in  $E_{\text{right}}(H)$ . Therefore, the vertex  $\text{new}_e$  is a subdivision vertex of the edge  $e$ . More formally,

$$\begin{aligned} V(H) &= V(G) \cup \{\text{new}_e \mid e \in E_{\text{cross}}(G)\}; \\ E(H) &= E_{\text{left}}(G) \cup E_{\text{right}}(G) \cup \{x \text{new}_e, \text{new}_e y \mid e = xy \in E_{\text{cross}}(G)\}. \end{aligned}$$

What did this achieve for us? The graph  $H$  has some nice properties, which we mentioned in item (c), and will elaborate now.

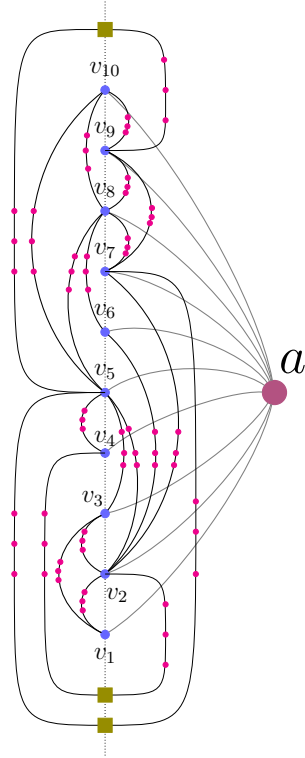


Figure 9: The graph  $H_{3\text{-div}}^{\text{apex}}$ , constructed from the the graph  $G$  shown in Figure 8(a). Note that  $H$  is obtained from  $G$  by introducing three new vertices (indicated by square nodes) by subdividing the three edges that cross the  $y$ -axis, namely  $v_2v_4$ ,  $v_5v_7$  and  $v_5v_9$ . The graph  $G_{7\text{-div}}^{\text{apex}}$  is then obtained from  $H_{3\text{-div}}^{\text{apex}}$  by introducing 4 additional subdivision vertices for all edges  $v_iv_j$  of  $G$  (except  $v_2v_4$ ,  $v_5v_7$  and  $v_5v_9$ ).

- $H$  is a subdivision of  $G$ . Edges of  $E_{\text{left}}(G)$  and  $E_{\text{right}}(G)$  are retained as-is in  $H$ , and edges of  $E_{\text{cross}}(G)$  are subdivided once.
- $H$  is a planar graph. This is because  $G$  is a planar graph, and subdivision does not affect planarity.
- No edge of  $H$  crosses the  $y$ -axis ( $E_{\text{cross}}(H) = \emptyset$ ). This is a straightforward feature of our construction.
- $n \leq n_H \leq 4n$ , where  $n_H = |V(H)|$ . This is because  $G$  has at most  $3n$  edges (as  $G$  is planar), and each edge of  $G$  is subdivided at most once in  $H$ . Since  $H$  also retains the vertices of  $G$ ,  $n_H \leq n + 3n$ .

From  $H$ , we construct  $H_{3\text{-div}}^{\text{apex}}$ , as described in Section 3.1. Then we progressively build its STABGIG representation (item (d)). We first define the positions of the segments corresponding to the apex vertex of  $H_{3\text{-div}}^{\text{apex}}$  and the original vertices of  $H$  in our STABGIG representation of  $H_{3\text{-div}}^{\text{apex}}$ . Note that the apex vertex in  $H_{3\text{-div}}^{\text{apex}}$  is called  $a$ , just as the apex vertex in  $G_k^{\text{apex}}$ , since these vertices finally coincide in our construction.

The vertices with the minimum and maximum  $y$ -coordinates in  $H$  are at  $(0, Y_{\min})$  and  $(0, Y_{\max})$ , where

$$Y_{\min} = \min(\{0\} \cup \{Y_e \mid e \in E_{\text{cross}}(G)\});$$

$$Y_{\max} = \max(\{n-1\} \cup \{Y_e \mid e \in E_{\text{cross}}(G)\}).$$

We may assume that  $Y_{\min} = 0$  and  $Y_{\max} = n_H - 1$ , and that the other vertices of  $H$  can be shifted accordingly so that their coordinates are  $(0, 0), (0, 1), (0, 2), \dots, (0, n_H - 1)$ .<sup>3</sup> Furthermore, the vertices are suitably renamed as  $w_1, w_2, w_3, \dots, w_{n_H}$  so that each  $w_i$  has the coordinate  $(0, i - 1)$ . For each vertex

<sup>3</sup>This can be done, for example, by shifting the  $x$ -axis downwards and making the gap between consecutive points as 1.

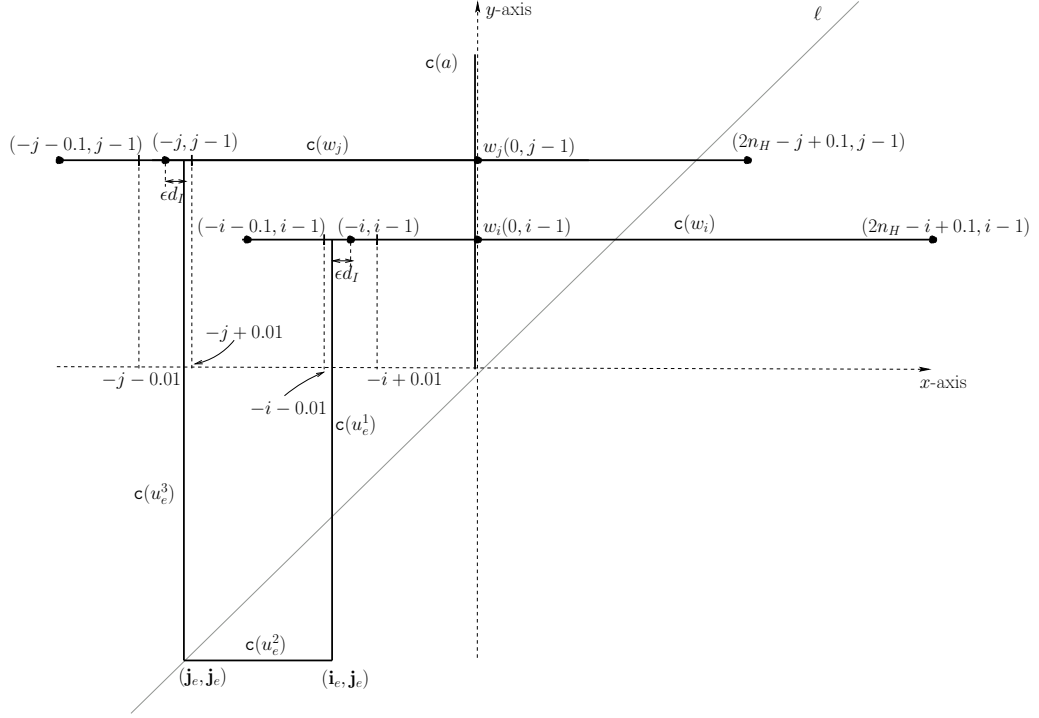


Figure 10: STABGIG representation of the path  $(w_i, u_e^1, u_e^2, u_e^3, w_j)$  of  $H_{3\text{-div}}^{\text{apex}}$  corresponding to the edge  $e = w_i w_j$  of  $H$ , with  $i < j$ .

$x \in V(H_{3\text{-div}}^{\text{apex}})$ , let  $c(x)$  be its corresponding segment. See Figure 10.

The apex vertex  $a$  of  $H_{3\text{-div}}^{\text{apex}}$ :  $c(a) = [(0, 0), (0, n_H - 1)]$

The original vertices of  $H$ :  $c(w_i) = [(-i - 0.1, i - 1), (2n_H - i + 0.1, i - 1)] \quad \forall i \in [n_H]$ .

We fix the line  $y = x$  as our stab line  $\ell$  (recall that  $\ell$  does not need to be axis-parallel). It is easy to see that all the segments described so far intersect the stab line. This brings us to item (e), where we need to place the segments corresponding to the three subdivision vertices of  $e$  for each edge  $e$  of  $H$ .

Let us consider edges of  $E_{\text{left}}(H)$ . Later, we will deal with edges of  $E_{\text{right}}(H)$ . We construct a set of intervals  $\mathcal{J}_{\text{left}}$  from  $E_{\text{left}}(H)$  as follows. For each edge  $e = w_i w_j \in E_{\text{left}}(H)$  (where  $i < j$ ), the set  $\mathcal{J}_{\text{left}}$  contains an open interval  $(i - 1, j - 1)$ . Thus, the number of intervals in  $\mathcal{J}_{\text{left}}$  is the number of edges in  $E_{\text{left}}(H)$ . Now, note that  $\mathcal{J}_{\text{left}}$  has the following interesting property.

**Observation 10.** *If two intervals of  $\mathcal{J}_{\text{left}}$  have an overlap (i.e., the intervals are not disjoint), then one of them must be contained in the other.*

Observation 10 is well known and easy to see; it is the basic underlying principle of *book thickness* or *book embeddings* of graphs (for a proof, see [6]). We will use this observation crucially in our construction of the three subdivision segments for each edge  $e$  of  $E_{\text{left}}(H)$ .

Given an interval  $I \in \mathcal{J}_{\text{left}}$ , let its *depth*, denoted by  $d_I$ , be the number of intervals  $I' \in E_{\text{left}}(H)$  such that  $I \subseteq I'$ . In other words,  $d_I$  is the number of intervals that contain  $I$  (including  $I$  itself). Thus,  $1 \leq d_I \leq n_H - 1$ . Now we are ready to describe our construction.

Fix  $\varepsilon = 0.01/n_H$ . Let  $e = w_i w_j \in E_{\text{left}}(H)$  such that  $i < j$ . Let  $I = (i - 1, j - 1)$  be the interval corresponding to  $e$  in  $\mathcal{J}_{\text{left}}$ . After the 3-subdivision, the edge  $e$  becomes the path  $(w_i, u_e^1, u_e^2, u_e^3, w_j)$  in  $H_{3\text{-div}}^{\text{apex}}$ . We already know the coordinates of the segments for  $w_i$  and  $w_j$ . As for the other three segments,

we define  $\mathbf{j}_e$  and  $\mathbf{i}_e$  as follows.

$$\begin{aligned}\mathbf{j}_e &= -j + \varepsilon \mathbf{d}_I; \\ \mathbf{i}_e &= -i - \varepsilon \mathbf{d}_I.\end{aligned}$$

Now, we are set to define the coordinates of the other three subdivision segments of  $e$ , which draw a  $\sqcup$ -shape. See Figure 10.

$$\begin{aligned}\mathbf{c}(u_e^3) &= [(\mathbf{j}_e, j - 1), (\mathbf{j}_e, \mathbf{j}_e)]; \\ \mathbf{c}(u_e^2) &= [(\mathbf{j}_e, \mathbf{j}_e), (\mathbf{i}_e, \mathbf{j}_e)]; \\ \mathbf{c}(u_e^1) &= [(\mathbf{i}_e, \mathbf{j}_e), (\mathbf{i}_e, i - 1)].\end{aligned}$$

Before proving that the 3 segments do not intersect any segments apart from  $w_i$ ,  $w_j$ , and each other, let us prove that all 3 segments intersect the stab line. Consider the point of intersection of  $\mathbf{c}(u_e^3)$  and  $\mathbf{c}(u_e^2)$ , namely  $(\mathbf{j}_e, \mathbf{j}_e)$ . This point has the same x- and y-coordinate, and so it lies on the stab line  $y = x$ . Thus, all that remains to be shown is that  $\mathbf{c}(u_e^1)$  also intersects the stab line. Since  $i \leq j - 1$  and  $\varepsilon \mathbf{d}_I < 0.01$ ,

$$\mathbf{j}_e \leq \mathbf{i}_e \leq i - 1.$$

Hence, the point  $(\mathbf{i}_e, \mathbf{i}_e)$  lies on the segment  $\mathbf{c}(u_e^1) = ((\mathbf{i}_e, \mathbf{j}_e), (\mathbf{i}_e, i - 1))$ , and on the stab line  $y = x$  also.

Now, we will show that for two edges  $e = w_i w_j$  (where  $i < j$ ) and  $e' = w_{i'} w_{j'}$  (where  $i' < j'$ ) of  $E_{\text{left}}(H)$ , the segments corresponding to the three subdivision vertices of  $e$  do not intersect the segments corresponding to the three subdivision vertices of  $e'$ . Let their corresponding intervals in  $\mathcal{J}_{\text{left}}$  be  $I$  and  $I'$ , respectively. Due to Observation 10, we have only two cases.

1. Case 1:  $I$  and  $I'$  are disjoint. Suppose that  $i < j \leq i' < j'$  (the other sub-case,  $i' < j' \leq i < j$ , is similar). We have the following.

$$\begin{aligned}i &< j \leq i' < j' \\ -j' &< -i' \leq -j < -i \\ -j' + \varepsilon \mathbf{d}_{I'} &< -i' - \varepsilon \mathbf{d}_{I'} < -j + \varepsilon \mathbf{d}_I < -i - \varepsilon \mathbf{d}_I \quad (\text{since } 2\varepsilon \mathbf{d}_{I'} < 1 \leq j' - i' \text{ and } 2\varepsilon \mathbf{d}_I < 1 \leq j - i) \\ \mathbf{j}_{e'} &< \mathbf{i}_{e'} < \mathbf{j}_e < \mathbf{i}_e\end{aligned}$$

Thus, the x-coordinate of each of the 3 subdivision segments of  $e'$  is at most  $\mathbf{i}_{e'}$ , and the x-coordinate of each of the 3 subdivision segments of  $e$  is at least  $\mathbf{j}_e$ . This completes the proof of Case 1.

2. Case 2: One of  $I$  or  $I'$  contains the other. Suppose that  $I \subseteq I'$  (the other sub-case,  $I' \subseteq I$ , is similar). Then, note that  $\mathbf{d}_{I'} < \mathbf{d}_I$ . We have the following.

$$\begin{aligned}i' &\leq i < j \leq j' && (\text{since } I \subseteq I') \\ -j' &\leq -j < -i \leq -i' \\ -j' + \varepsilon \mathbf{d}_{I'} &< -j + \varepsilon \mathbf{d}_I < -i - \varepsilon \mathbf{d}_I < -i' - \varepsilon \mathbf{d}_{I'} && (\text{since } \mathbf{d}_{I'} < \mathbf{d}_I \text{ and } 2\varepsilon \mathbf{d}_I < 1 \leq j - i) \\ \mathbf{j}_{e'} &< \mathbf{j}_e < \mathbf{i}_e < \mathbf{i}_{e'}\end{aligned}$$

Thus, the x-coordinate of  $\mathbf{c}(u_{e'}^3)$  (namely  $\mathbf{j}_{e'}$ ) is less than the x-coordinate of each of the 3 subdivision segments of  $e$ , and the x-coordinate of  $\mathbf{c}(u_{e'}^1)$  (namely  $\mathbf{i}_{e'}$ ) is greater than the x-coordinate of each of the 3 subdivision segments of  $e$ . Finally, the y-coordinate of  $\mathbf{c}(u_{e'}^2)$  (namely  $\mathbf{j}_{e'}$ ) is less than the y-coordinate of each of the 3 subdivision segments of  $e$ . This completes the proof of Case 2.

This completes the construction of the STABGIG representation for the subgraph of  $H_{3\text{-div}}^{\text{apex}}$  induced by the original vertices of  $H$ , the apex vertex  $a$  and the subdivision vertices located in the left half-plane.

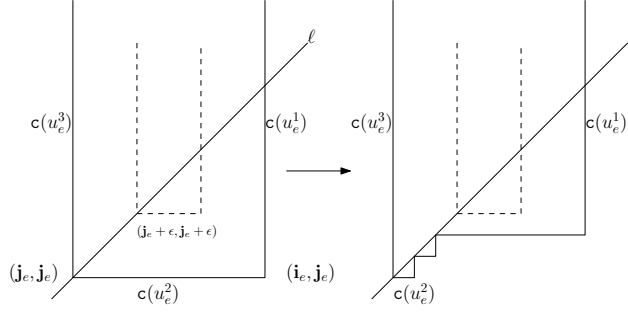


Figure 11: Replacement of  $c(u_e^2)$  (left), for some edge  $e$  which is not sufficiently subdivided in  $H_{3\text{-div}}^{\text{apex}}$ , with a sequence of segments describing a path of length  $2h + 1$  (right). In this figure,  $h = 2$ . The dotted  $\sqsubset$ -shape indicates the closest possible location of an  $\sqsubset$ -shape located above the one we defined for  $e$ .

For the vertices and edges located in the right half-plane, the construction is similar but replaces the  $\sqsubset$ -shapes by  $\sqsupset$ -shapes. The correctness of our construction follows from Cases 1 and 2 above.

### 3.2.3 STABGIG representation of $G_{k\text{-div}}^{\text{apex}}$

In order to conclude our proof of Proposition 9, we need – according to item (f) – to convert the STABGIG representation of  $H_{k\text{-div}}^{\text{apex}}$  into a STABGIG representation of  $G_{k\text{-div}}^{\text{apex}}$ , for an arbitrary  $k \geq 7$ . This operation reduces to further subdividing one edge of  $H_{3\text{-div}}^{\text{apex}}$ , that may be appropriately chosen, by transforming it into a path of odd length  $2h + 1$ , for an appropriate integer  $h \geq 1$ .

Consider the STABGIG representation of  $H_{3\text{-div}}^{\text{apex}}$ . For each edge  $e \in E_{\text{cross}}(G)$ , a 7-subdivision is performed in  $H_{3\text{-div}}^{\text{apex}}$ . But for each edge  $e \in E_{\text{left}}(G) \cup E_{\text{right}}(G)$ , only a 3-subdivision is performed in  $H_{3\text{-div}}^{\text{apex}}$ . When  $k = 7$ , the latter edges are insufficiently subdivided in  $H_{3\text{-div}}^{\text{apex}}$  with respect to  $G_{k\text{-div}}^{\text{apex}}$ . Moreover, when  $k > 7$  all the original edges in  $G$  are insufficiently subdivided. In all cases, let  $e \in E(G)$  be one of the edges that are insufficiently subdivided, and assume that  $e \in E_{\text{left}}(H)$ . (Otherwise, when  $e \in E_{\text{right}}(H)$  the approach is similar, whereas when  $e \in E_{\text{cross}}(G)$  we have to perform the same approach on the 'half-edge' of  $e$  that belongs to  $E_{\text{left}}(H)$ .) In  $H_{3\text{-div}}^{\text{apex}}$ ,  $e$  is 3-subdivided. Assume we need a  $k$ -subdivision of  $e$ , with odd  $k \geq 7$ , and let  $h = (k - 3)/2$ . Then we perform a  $2h$ -subdivision of the edge  $u_e^1 u_e^2$  of  $H_{3\text{-div}}^{\text{apex}}$ , and describe below the new segments representing  $u_e^1, u_e^2$  and the  $2h$  supplementary vertices.

In  $H_{3\text{-div}}^{\text{apex}}$ , the intersection point between the segments  $c(u_e^3)$  and  $c(u_e^2)$  is  $(\mathbf{j}_e, \mathbf{j}_e)$ . The closest possible similar point located on the stab line towards right is the point  $(\mathbf{j}_e + \varepsilon, \mathbf{j}_e + \varepsilon)$ . We then replace the segment  $c(u_e^2)$  with a succession of  $2h + 1$  alternating horizontal and vertical segments whose intersections define the path required by the  $2h$ -subdivision of  $(u_e^1, u_e^2)$ . See Figure 11.

Formally, let  $\varepsilon_2 = \varepsilon/(h + 1)$ , and define the following segments. The horizontal segment obtained for  $h = 0$  is the new segment  $c(u_e^2)$ .

For  $0 \leq t \leq h - 1$ :

$$\begin{aligned} & [(\mathbf{j}_e + t\varepsilon_2, \mathbf{j}_e + t\varepsilon_2), (\mathbf{j}_e + (t + 1)\varepsilon_2, \mathbf{j}_e + t\varepsilon_2)] \\ & [(\mathbf{j}_e + (t + 1)\varepsilon_2, \mathbf{j}_e + t\varepsilon_2), (\mathbf{j}_e + (t + 1)\varepsilon_2, \mathbf{j}_e + (t + 1)\varepsilon_2)] \end{aligned}$$

Complete this set of segments with:

$$\begin{aligned} & [(\mathbf{j}_e + h\varepsilon_2, \mathbf{j}_e + h\varepsilon_2), (\mathbf{i}_e, \mathbf{j}_e + h\varepsilon_2)] \\ & c(u_e^1) = [(\mathbf{i}_e, \mathbf{j}_e + h\varepsilon_2), (\mathbf{i}_e, i - 1)] \end{aligned}$$

All the segments corresponding to the  $2h$  new subdivision vertices lie strictly below the closest upper segment not involved in the subdivision of  $e$  (whose  $y$ -coordinate is at least  $\mathbf{j}_e + \varepsilon$ ), and (not strictly)

above the former segment  $c(u_e^2)$ . They also lie between the  $x$ -coordinates of  $c(u_e^3)$  and  $c(u_e^1)$ . Thus they cannot intersect other segments. So we have representation of the path with  $(2h + 1)$  edges required by the subdivision.

This ends the proof of Proposition 9.

### 3.2.4 Proof of Theorem 2

For a given graph  $\Gamma$ , recall (see Section 2.2) that  $\Gamma + x$  is the graph obtained by adding to  $\Gamma$  a universal vertex  $x$ . In order to show that STABGIGREC belongs to NP, note that a grid representation of  $\Gamma$  in which all the segments are stabbed by the same line  $\ell$  may be seen as a representation in the plane of  $\Gamma + x$  with segments following at most three directions ( $x$  is represented by the stab line  $\ell$ , that is replaced in this representation with a long segment). This remark allows us to invoke once again the result in [20], which guarantees that since the number of directions of the segments in the representation is fixed, STABGIGREC is in NP.

Furthermore,  $G_{k\text{-div}}^{\text{apex}}$  is obtained in polynomial time from  $G$ . According to Observation 7 with fixed  $k \geq 7$  and  $g = k + 3$ , the girth of  $G_{k\text{-div}}^{\text{apex}}$  equals  $g$ . It remains to show that  $G$  is a yes-instance of PHPC if and only if  $G_{k\text{-div}}^{\text{apex}}$  is a yes-instance of STABGIGREC. Proposition 9 shows the forward direction.

For the backward direction, we first show – seeking to use Proposition 8 – that if  $G_{k\text{-div}}^{\text{apex}}$  is a STABGIG, then  $G_{k\text{-div}}^{\text{apex}}$  is a 1-string graph. To this end, it is sufficient to note that each segment in a grid representation of  $G_{k\text{-div}}^{\text{apex}}$  is a 1-string, and that two segments that intersect without crossing (because an endpoint of one segment lies on the second segment) may be easily transformed into two crossing segments. Now, using Proposition 8, we deduce that  $G$  is a yes-instance of PHPC.

## 4 Conclusion

In this paper, we proved that recognizing grounded L-graphs is NP-complete. A natural direction of research would be to find interesting subclasses of grounded L-graphs with polynomial time recognition algorithms. One such candidate class could be the *grounded unit L-graphs*. A unit L-shape is a made by joining the bottom end-point of a vertical (|) segment (of arbitrary length) to the left end-point of a horizontal (–) segment of *unit* length. Grounded unit L-graphs are the intersection graphs of unit L-shapes such that all the L-shapes’ anchors lie on the same horizontal line. Grounded unit L-graphs is a subclass of *cocomparability* graphs and contains *unit interval* graphs and *permutation graphs* as its subclasses. The above discussion motivates the following question.

**Question 1.** *What is the computational complexity of recognizing grounded unit L-graphs?*

In this paper, we proved that recognizing stabbable grid intersection graphs is NP-complete even when the inputs are restricted to apex graphs, a graph class that does not contain  $K_6$  as a minor. In contrast, recognizing  $K_4$ -minor free stabbable grid intersection graphs is trivial (since  $K_4$ -minor free graphs are planar and all planar bipartite graphs are stabbable grid intersection graphs). This motivates the following question.

**Question 2.** *What is the computational complexity of recognizing  $K_5$ -minor free stabbable grid intersection graphs?*

Theorem 2 implies that STABGIGREC is not FPT (fixed-parameter tractable), when parameterized by the *apex number* of the graph, that is, the minimum number of vertices required to be removed to make the resultant graph planar. But our reduction procedure results in graphs with large maximum degree. On the other hand, a result of Mustařă & Pergel [24], implies that recognizing many geometric intersection graph classes (e.g. string graphs, 1-string graphs) remain NP-hard even if the maximum degree of the input graph is bounded by a constant. Therefore, recognition of such graph classes does not admit FPT with respect to the maximum degree. But the graphs produced by their reduction procedure have large apex number. Therefore, the following question arises.

**Question 3.** *Is STABGIGREC FPT w.r.t sum of maximum degree and apex number?*



## References

- [1] Pankaj K Agarwal, Marc Van Kreveld, and Subhash Suri. Label placement by maximum independent set in rectangles. *Computational Geometry*, 11(3-4):209–218, 1998.
- [2] Andrei Asinowski, Elad Cohen, Martin Charles Golumbic, Vincent Limouzy, Marina Lipshteyn, and Michal Stern. Vertex intersection graphs of paths on a grid. *J. Graph Algorithms Appl.*, 16(2):129–150, 2012.
- [3] E Asplund and B Grünbaum. On a coloring problem. *MATHEMATICA SCANDINAVICA*, 8:181–188, 1960.
- [4] C. Auer and A. Gleißner. Characterizations of deque and queue graphs. In *International Workshop on Graph-Theoretic Concepts in Computer Science*, pages 35–46. Springer, 2011.
- [5] Seymour Benzer. On the topology of the genetic fine structure. *Proceedings of the National Academy of Sciences*, 45(11):1607–1620, 1959.
- [6] Frank Bernhart and Paul C Kainen. The book thickness of a graph. *Journal of Combinatorial Theory, Series B*, 27(3):320–331, 1979.
- [7] Prosenjit Bose, Paz Carmi, J Mark Keil, Anil Maheshwari, Saeed Mehrabi, Debajyoti Mondal, and Michiel Smid. Computing maximum independent set on outerstring graphs and their relatives. *Computational Geometry*, 103:101852, 2022.
- [8] Dibyayan Chakraborty, Sandip Das, and Joydeep Mukherjee. On dominating set of some subclasses of string graphs. *Computational Geometry*, 107:101884, 2022.
- [9] Dibyayan Chakraborty and Kshitij Gajjar. Finding geometric representations of apex graphs is np-hard. In *International Conference and Workshops on Algorithms and Computation*, pages 161–174. Springer, 2022.
- [10] Steven Chaplick, Stefan Felsner, Udo Hoffmann, and Veit Wiechert. Grid intersection graphs and order dimension. *Order*, 35(2):363–391, 2018.
- [11] F. Chung, F. T. Leighton, and A. Rosenberg. *Diogenes: A methodology for designing fault-tolerant VLSI processor arrays*. Department of Electrical Engineering and Computer Science, Massachusetts Institute of Technology, Microsystems Program Office, 1983.
- [12] Fan RK Chung, Frank Thomson Leighton, and Arnold L Rosenberg. Embedding graphs in books: a layout problem with applications to vlsi design. *SIAM Journal on Algebraic Discrete Methods*, 8(1):33–58, 1987.
- [13] James Davies, Tomasz Krawczyk, Rose McCarty, and Bartosz Walczak. Grounded L-graphs are polynomially  $\chi$ -bounded. *arXiv preprint arXiv:2108.05611*, 2021.
- [14] Stefan Felsner. Rectangle and square representations of planar graphs. In *Thirty essays on geometric graph theory*, pages 213–248. Springer, 2013.
- [15] Daniel Gonçalves, Lucas Isenmann, and Claire Pennarun. Planar graphs as L-intersection or L-contact graphs. In *Proceedings of the Twenty-Ninth Annual ACM-SIAM Symposium on Discrete Algorithms*, pages 172–184, 2018.
- [16] András Gyárfás and Jenő Lehel. Covering and coloring problems for relatives of intervals. *Discrete Mathematics*, 55(2):167–180, 1985.
- [17] I. B. Hartman, I. Newman, and R. Ziv. On grid intersection graphs. *Discrete Mathematics*, 87(1):41–52, 1991.

- [18] Vít Jelínek and Martin Töpfer. On grounded L-graphs and their relatives. *The Electronic Journal of Combinatorics*, pages P3–17, 2019.
- [19] J. Kratochvíl. A special planar satisfiability problem and a consequence of its NP-completeness. *Discrete Applied Mathematics*, 52(3):233–252, 1994.
- [20] Jan Kratochvíl and Jirí Matousek. Intersection graphs of segments. *Journal of Combinatorial Theory, Series B*, 62(2):289–315, 1994.
- [21] F. Kuhn, R. Wattenhofer, and A. Zollinger. Ad hoc networks beyond unit disk graphs. *Wireless Networks*, 14(5):715–729, 2008.
- [22] C Lekkeikerker and Johan Boland. Representation of a finite graph by a set of intervals on the real line. *Fundamenta Mathematicae*, 51:45–64, 1962.
- [23] Sean McGuinness. On bounding the chromatic number of L-graphs. *Discrete Mathematics*, 154(1-3):179–187, 1996.
- [24] I. Mustață and M. Pergel. On unit grid intersection graphs and several other intersection graph classes. *Acta Mathematica Universitatis Comenianae*, 88(3):967–972, 2019.
- [25] Irena Rusu. On the complexity of recognizing Stick graphs. *preprint arXiv:2205.09076*, 2022.
- [26] N. A. Sherwani. *Algorithms for VLSI Physical Design Automation*. Springer US, 2007.
- [27] D. M. Thilikos and H. L. Bodlaender. Fast partitioning L-apex graphs with applications to approximating maximum induced-subgraph problems. *Information processing letters*, 61(5):227–232, 1997.
- [28] D. J. A. Welsh. Knots and braids: some algorithmic questions. *Contemporary Mathematics*, 147, 1993.
- [29] J. Xu and B. Berger. Fast and accurate algorithms for protein side-chain packing. *Journal of the ACM (JACM)*, 53(4):533–557, 2006.